5

Nina Gartner, Miha Hren, Tadeja Kosec, Andraž Legat

Electrochemical corrosion tests on steel in alkali-activated materials

ELECTROCHEMICAL CORROSION TESTS ON STEEL IN ALKALI-ACTIVATED MATERIALS

N. Gartner[1], M. Hren[1], T. Kosec[1] and A. Legat[1]

[1] Slovenian Nationa Building and Civil Engineering Institute, Department of Materials
Dimiceva ul. 12, 1000 Ljubljana
e-mail: nina.gartner@zag.si

SUMMARY: One of the potential alternatives to Ordinary Portland Cement (OPC) are Alkali-Activated Materials (AAMs). The service life of reinforced concrete structures greatly depends on the corrosion resistance of embedded steel reinforcement. Due to the wide range of AAMs and their diverse properties, corrosion processes of steel in these materials are relatively unknown. Corrosion monitoring methods or their interpretations in certain cases cannot be directly transferred from the ones for OPC materials. The chemical compositions of pore solution in different AAMs influence the results of electrochemical measurements and their interpretations. Within this research, three different alkali-activated mortar mixes were prepared, based on fly ash, slag or metakaolin. Pore solutions were extracted from each mortar and chemical analysis was acquired. Different electrochemical corrosion measurements were performed on steel submerged to synthetic pore solutions. In parallel, ordinary carbon steel reinforcing bar was installed in the same types of alkali-activated mortar mixes. Specimens were exposed to wet/dry cycles with saline solution and periodic measurements of electrochemical impedance spectroscopy (EIS) were performed. Measured parameters in both systems were analysed and compared. It was concluded that electrochemical measurements in pore solutions can provide basic overview on corrosion behaviour in different AAMs environments. Periodic EIS measurements enabled monitoring of corrosion initiation and propagation on steel reinforcement in AAMs, although the information on the corrosion type is missing. Interpretation of results depends on visual analysis of corrosion damages after the end of exposure, providing information on corrosion type and intensity. The continuation of research on corrosion monitoring techniques will be performed by using Electrical Resistance (ER) sensors and Coupled Multi-Electrode Array (CMEA) sensors.

KEY WORDS: corrosion, alkali-activated mortars, pore solution extraction, electrochemical corrosion techniques, visual analysis;

1 INTRODUCTION

Concrete is the most widely used man-made building material in the world. During the production of its main component, ordinary Portland cement (OPC), the estimated 5–8 % of global anthropogenic CO_2 emissions are released [1,2]. Alkali-Activated Materials (AAMs) use supplementary cementitious materials (SCMs) as a total replacement of OPC and are one of the potential alternatives to OPC containing binders for a wide range of possible applications [3,4]. AAMs are formed by the reaction between various aluminosilicate precursors, often in the form of industrial by-products, and alkaline activators. Wide range of combinations form materials with various properties and applicabilities [4]. The use of AAMs for reinforced concrete elements raises the issue of steel corrosion, which is the main cause of their premature failure. The loss of alkalinity and the ingress of chloride ions are the primary causes of steel corrosion in OPC concrete [2]. However, the pore solutions in AAMs can significantly differ from OPC-based cements in terms of their chemical, mineralogical and redox characteristics [5], which can strongly influence all phases of corrosion process and causing difficulties with interpretation of parameters obtained by electrochemical tests usually used for corrosion tests in cementitious materials. The difference between corrosion processes in concrete mixes (also alkali-activated materials) and solutions is that the anodic and cathodic sites are spatially localized due to the porous and inhomogeneous structure of the concrete [6]. Therefore, information on corrosion rate in concrete should contain information on corrosion type, i.e. if it is placed uniformly across the surface or it is more localized. Commonly used electrochemical monitoring techniques, such as electrochemical impedance spectroscopy [7], potentiodynamic polarization tests, or linear polarisation resistance measurements, generally do not differentiate between general and localized corrosion and the corrosion damage can only be evaluated when steel is destructively removed from the concrete. The aim of this paper is to evaluate electrochemical methods for testing steel corrosion in different AAM mixes and in their pore solutions, and to compare the results obtained in both environments.

2 MATERIALS AND METHODS

2.1 Experiments in Alkali-Activated Mortars

Mortar mix-designs used in this research were developed by RILEM TC 247-DTA, which was aiming at development of recommendations for durability testing of alkali-activated materials [8–11]. Three types of mortars designed for assessing the sulphate resistance were selected, based on three different precursors, i.e. fly-ash (FA8), steel slag (S3a-661) and metakaolin (MK2). The exact mortar mixture designs are presented in Table 1.

Compressive strength [12] measured after 56 days on tested mortars were: MK2 (70 MPa) > S3a-661 (60 MPa) > FA8 (39 MPa). The results of Hg porosimetry showed the following proportion of pores in tested mortars: FA8 (15 %) > MK2 (14 %) > S3a-661 (11 %).

Table 1: Mortar mix-designs used in this study [8–11].

Mortar / [g]	**FA8**	**S3a-661**	**MK2**
Flay ash (V-378/14)	455.9	-	-
Slag (V-138/15)	-	557.4	-
Metakaolin (V-63/15)	-	-	450.0
Water glass (V-25/15)	168.5	22.4	-
Water glass (V-502/14)	-	-	372.0
NaOH (V-44/15)	-	33.4	37.8
NaOH solution 41.7 % (wt.) NaOH + 58.3 % (wt.) H2O	64.4	-	-
Tap water	17.7	232.3	5.0
CEN Standard sand (EN 196-1)	1350.0	1350.0	1350.0

Three parallel specimens for each mortar mix were prepared for corrosion tests. Specimens were cast in prism shaped moulds in dimensions of 3×3×10 cm^3. Cold ribbed steel reinforcing bar type B 500B (1.0439 [13]) with diameter Φ6 mm was embedded in each specimen. Both ends of steel bar were protected with epoxy based coating in a way that the length of 9 cm in the middle was unprotected and the surface area of 17 cm^2 was exposed to mortar. Steel bar was covered with 7 mm mortar cover. After casting specimens were cured in humidity chamber for 28 days. After curing specimens were exposed to wetting / drying cycles with 3.5 % of NaCl solution from the pool on the top of each specimen. One cycle was one week long – 3 days of wetting and 4 days of drying.

Electrochemical Impedance Spectroscopy (EIS) measurements were performed once in each cycle, i.e. on the last day of wetting period. Steel reinforcing bar embedded in mortar specimen was used as working electrode, a graphite electrode and a saturated calomel electrode (SCE) submerged in top pool of the specimen served as the counter and reference electrode, respectively. The EIS measurements were performed using a Gamry Ref600 potentiostat. All potentials refer to the SCE scale. EIS measurements were performed at open circuit potential (OCP) in the frequency range from 65 kHz to 5 mHz with 11 points per decade and an amplitude of ±10 mV. The total impedance ($|Z|_{total}$) values were estimated as impedances ($|Z|$) at the lowest measured frequencies with deducted solution resistance (R_s) values.

j_{corr} values were calculated using the Stern-Geary equation; an estimated constant B = 0.026 V was used [14]. $|Z|_{total}$ was used as a near estimation for polarisation resistance (R_p) in calculations from EIS parameters. v_{corr} values were calculated according to Equation 1 [7] using atomic mass value AM = 55.85, Faraday constant F = 9.65 × 10^4 As, valence n = 2, and steel density ρ = 7.89 g/cm^3.

$$v_{corr} = \frac{AM \cdot j_{corr}}{n \cdot F \cdot \rho} \qquad \text{Equation 1}$$

At the end of exposure, mortar specimens were broken and visual inspection of corrosion damages on steel bars was performed by means of macroscopic images. Visual analysis was performed as a complementary method for verification of electrochemical measurements by determination of corrosion type and intensity.

2.2 Experiments in Alkali-Activated Mortar pore solutions

Three different AAMs mixes (Table 1) were cast in cylinder shaped moulds and cured in a sealed plastic foil. Due to insufficient humidity of mortar after 28 days of curing specimens were broken into smaller (approx. 3-4 cm) pieces and slowly re-wetted with drops of distilled water in a way that no extra water was left out of the mortar. After one day from drip-wetting, pore solutions were extracted from mortars with high-pressure device (up to 1000 MPa) [15,16]. Extracted pore solutions were further analysed for their pH and chemical composition using ion-exchange chromatography system 940 Professional IC Vario (Metrohm). Based on the results, simulated pore solutions were prepared. The pH was adjusted with the ratio of silicate in OH^- ions. Exact chemical compositions of simulated pore solutions are presented in Table 2.

Table 2: Chemical compositions of simulated pore solutions, prepared on the basis analysed pore solutions extracted from alkali-activated mortars (Table 1).

Mortar (Table 1)	**pH**	**Salts** [g/L]								
		NaCl	**KCl**	**K_2SO_4**	**Na_2SO_4**	**$NaNO_3$**	**Na_2HPO_4**	**NaOH**	**KOH**	**$Na_2Si_2O_5$** (72 wt.%)
FA8	12.36	0.053	-	1.502	22.871	-	7.859	2.081	-	79.968
S3a-661	12.52	-	0.400	0.914	-	-	-	1.430	1.805	196.486
MK2	12.37	0.054	-	0.089	0.275	0.646	-	5.840	-	184.670

Simulated pore solutions (Table 2) were used as the electrolyte for different electrochemical corrosion measurements. Experiments were performed in standard corrosion cell. The working electrodes were made of disc steel with surface area of 0.785 cm^2 and similar composition and microstructure to that used for the concrete reinforcement (Table 3). The tablets were polished before the experiments by means of SiC paper grit 600 and placed in ethanol ultrasonic bath. A graphite electrode served as the counter electrode, and a saturated calomel electrode (SCE) was used as the reference electrode.

Table 3: Chemical composition of steel sheet used as a working electrode in electrochemical measurements.

C [wt.%]	**P** [wt.%]	**S** [wt.%]	**Cu** [wt.%]	**N** [wt.%]	**C_{eq}** [wt.%]
0.14	0.008	0.012	0.073	0.006	0.23

Three electrochemical techniques were performed: linear polarisation resistance (LPR) measurements, electrochemical impedance spectroscopy (EIS) and cyclic potentiodynamic polarization (CPD) scans, in that sequence order. The LPR measurement was performed after 90 min stabilization in exposure environment. Measuring potential interval was set from –20 mV up to +20 mV at open-circuit potential (E_{oc}) measured before the measurement. The scan rate was 0.1 mV/s and sampling period was 1 s. The EIS measurement was performed at E_{oc}. The frequency range was set from 65 kHz to 5 mHz, measured 11 points per decade. The total impedance ($|Z|_{total}$) values were estimated as impedances ($|Z|$) at the lowest measured frequencies with deducted solution resistance (R_s) values. By means of CPD measurements, the polarization potential was scanned from −0.25 V vs. E_{oc} to +0.75 V vs. reference potential (E_{ref}) and back to −0.25 V vs. E_{oc}, with a scan rate 1 mV/s and sampling period 1 s.

j_{corr} values were calculated using the Stern-Geary equation and v_{corr} values were calculated according to Equation 1, with the same parameters as for measurements in mortars (see chapter 2.1.2). $|Z|_{total}$ was used in calculations as a near estimation for polarisation resistance (R_p).

3 RESULTS

3.1 Results in Alkali-Activated Mortars pore solutions

First, measurements were performed in three simulated AAM pore solutions (Table 2).

Linear polarisation resistance (LPR) showed small differences between measurements in different pore solutions. Polarisation resistance values are relatively high and represent corrosion rates lower than 1 μm/year.

Figure 1: Scattering of R_p values measured with LPR in AAMs pore solutions.

Electrochemical impedance spectroscopy (EIS) curves measured in simulated pore solution are presented as Nyquist and Bode plots (Figure 2). Impedance responses have similar shapes, but the lowest impedance values were measured on steel in S3a-661 (slag) pore solution, higher in FA8 (fly ash) pore solution and the highest in MK4 (metakaolin) pore solution. Parameters of total impedance ($|Z|_{total}$) and calculated corrosion rates (ν_{corr}) are presented in Table 4.

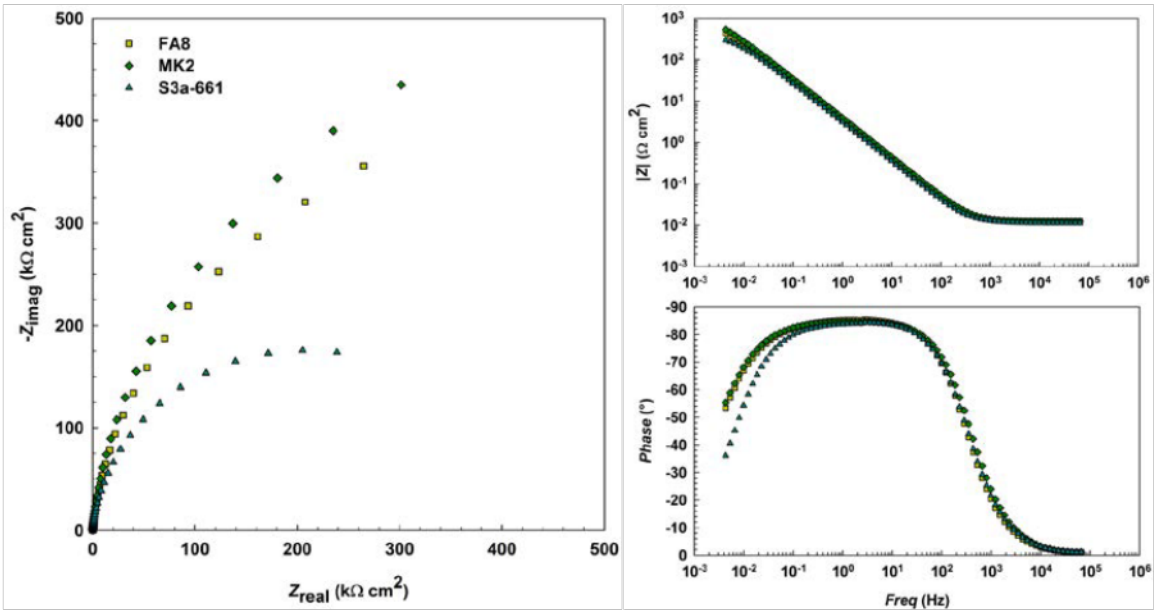

Figure 2: Representative EIS spectra recorded in three AAMs solutions.

Table 4: Total impedance ($|Z|$) values measured with EIS measurements and calculated corrosion rates (ν_{corr}) in different AAMs pore solutions.

AAM solution type	$\|Z\|_{total}$ [kΩ·cm^2]	ν_{corr} [μm/year]
FA8	412	0.7
S3a-661	326	0.9
MK2	545	0.6

Cyclic potentiodynamic polarization (CPD) scans measured on steel in different simulated pore solutions are presented in Figure 3. The shapes of CPD curves are similar in all pore solutions; steel exhibits pseudo positive region. After potential is reversed, negative hysteresis is observed, which indicates that pitting is not likely to occur. Measured current density (j_{corr}) is the lowest for steel in MK4 (metakaolin) pore solution, highest in FA8 (fly ash) pore solution and the highest in S3a-661 (slag) pore solution. Similar as in the case of EIS measurements, the MK4 pore solution represents the least corrosive environment.

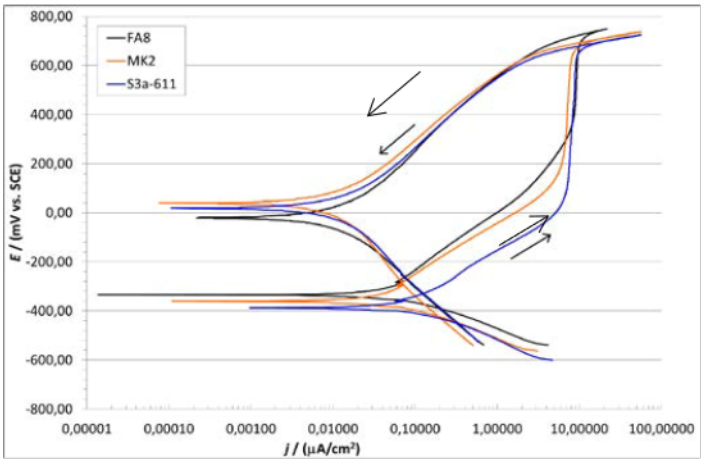

Figure 3: Representative CPD scans recorded in three AAMs solutions.

Table 5: Current density (j_{corr}) and corrosion potential (E_{corr}) values measured with EIS measurements and calculated corrosion rates (v_{corr}) in different AAMs pore solutions.

AAM solution type	E_{corr} [mV]	j_{corr} [µA/cm^2]	v_{corr} [µm/year]
FA8	–336	0.06	0.7
S3a-661	–365	0.09	1.0
MK2	–340	0.04	0.5

The corrosion rates were calculated from parameters measured with three different electrochemical methods: polarisation resistance (LPR) measurements, electrical impedance spectroscopy (EIS) and cyclic potentiodynamic polarization (CPD) scans. j_{corr} values were calculated using the Stern-Geary equation and v_{corr} values were calculated according to Equation 1, as described in Experimental. All three electrochemical methods show very similar results (Table 6), with very low corrosion rates below 1 µm/year. The highest corrosion rates were measured in S3a-661 (slag) and the lowest in MK2 (metakaolin) mortar pore solution.

Table 6: Calculated corrosion rates (v_{corr}) in three different AAMs pore solutions with three different electrochemical techniques: LPR, EIS and CPD.

AAM solution type	LPR v_{corr} [µm/year]	EIS v_{corr} [µm/year]	CPD v_{corr} [µm/year]
FA8	0.5	0.7	0.7
S3a-661	0.8	0.9	1.0
MK2	0.3	0.6	0.5

3.2 Results in Alkali-Activated Mortars

Electrochemical impedance spectroscopy (EIS) measurements were periodically performed during wetting/drying cycles on steel reinforcement bars embedded in three alkali-activated mortar (AAM) mixes (Table 1). Spectra show (Figure 4 and Figure 5) that shapes differ among different mortars and also change significantly during the exposure period. The resistance of exposure media (mortar) increases with each cycle.

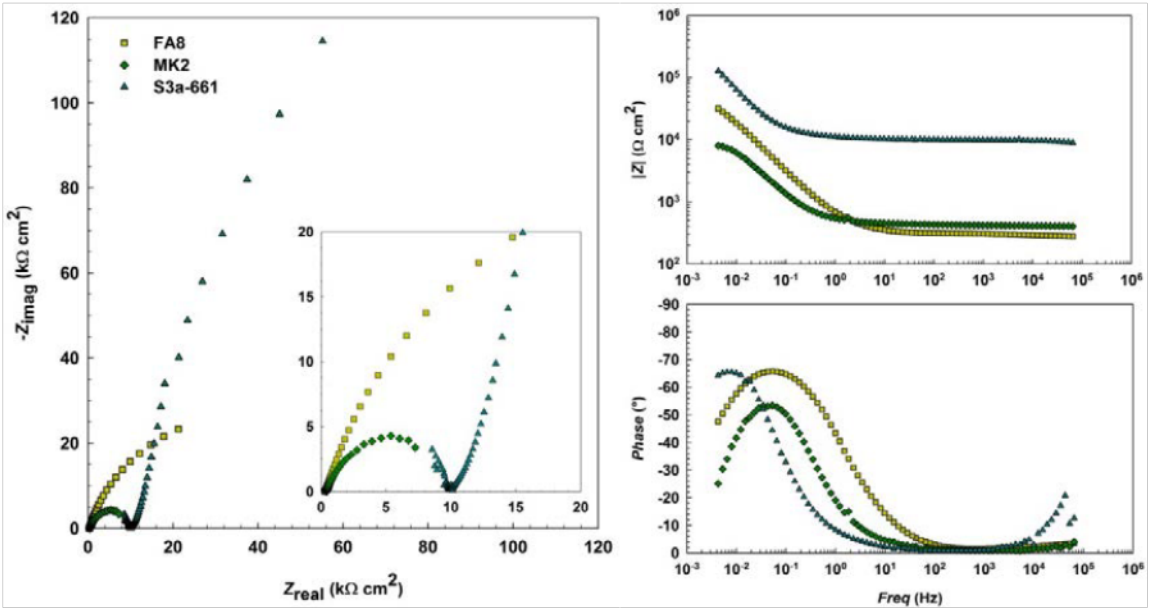

Figure 4: Representative EIS spectra recorded in 1st wetting / drying cycle in three alkali-activated mortars.

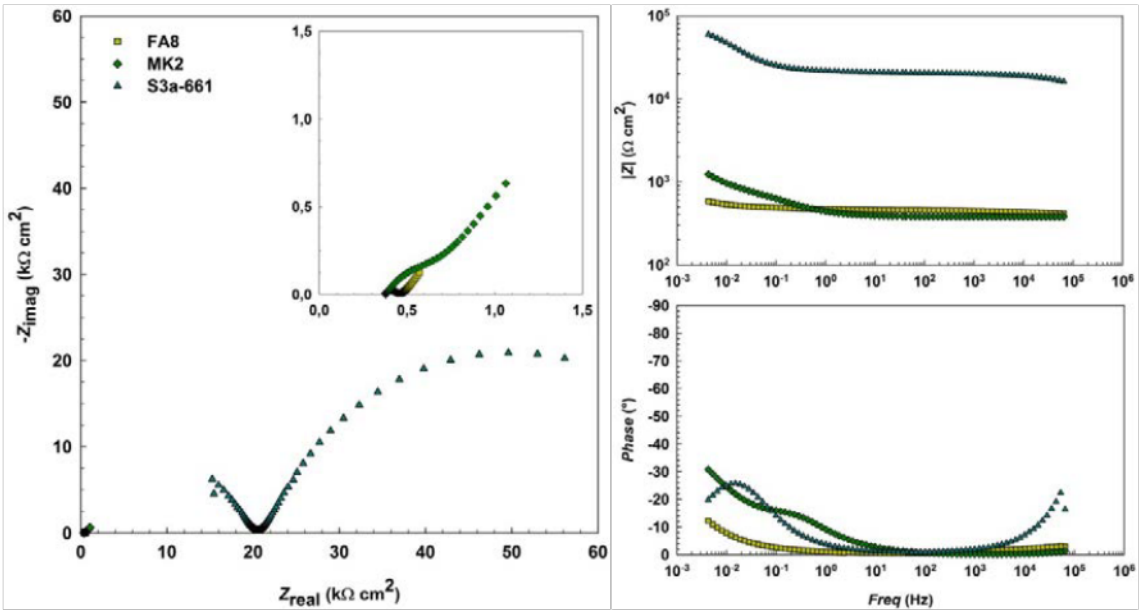

Figure 5: Representative EIS spectra recorded in 17th wetting / drying cycle in three alkali-activated mortars.

Values of total impedance ($|Z|_{total}$) measured in mortar are significantly lower from values measured in pore solutions; consequently, corrosion rates (ν_{corr}) are higher already from initial measurements (Table 7). The corrosion processes intensify over time of exposure, since measured parameters of total impedance ($|Z|_{total}$) values and consequently corrosion rates (ν_{corr}) are increasing with time (Table 7). This is expected due to the presence of Cl^- ions in mortar which are increasing by each cyclic wetting with 3.5 % NaCl solution. The measured rise of ν_{corr} is especially high in FA8 mortar, where values gradually go from 10 μm/year in the 1st wetting/drying cycle to 2400 μm/year in 17th cycle. The increase of ν_{corr} values measured in MK2 mortar is lower (from 40 μm/year to 350 μm/year in 17 cycles), but significant. However, steel embedded in S3a-661 mortar is still not experiencing significant corrosion rates after 17 cycles of exposure (ν_{corr} is up to 8 μm/year).

Contrary to measurements in pore solution, electrochemical impedance spectroscopy (EIS) curves also show shapes which differ among different mortars and change significantly during the exposure period (Figure 4 and Figure 5). The resistance of exposure media (mortar) is also rising with each cycle.

Table 7: Total impedance ($|Z|_{total}$) values measured with EIS measurements and calculated corrosion rates (ν_{corr}) in different alkali-activated mortars.

AAM solution type	$\|Z\|_{total}$ [kΩ·cm^2]		ν_{corr} [μm/year]	
	Week 1	Week 17	Week 1	Week 17
FA8	31	0.1	10	2400
S3a-661	117	39	3	8
MK2	8	857	40	350

After 17 weeks of exposure, mortar specimens were demolished and steel bars were analysed. Visual inspection of steel bars (Figure 6) confirmed the intensity of corrosion activities measured with electrochemical impedance spectroscopy (EIS) technique. Images of steel bar embedded in FA8 (fly ash) mortar (Figure 6a) show severe corrosion damages – surface is rough due to local pits merged together in large areas of corrosion damages with visible reduction of rebar diameter. Damages on steel bar embedded in MK2 mortar (Figure 6b) are clearly visible and locally fairly deep. However, damages on steel bar embedded in S3a-661 mortar (Figure 6c) are very few and shallow, limited to edge areas. As seen from Figure 6 the comparison of visual damages corresponds with EIS results, which indicate the highest corrosion rates on steel in FA8 mortar, significant corrosion rates on steel in MK2 mortar and very low corrosion rates on steel in S3a-661 mortar. However, considering real area of corrosion damages, calculated local corrosion rates would be even higher.

Figure 6: Corrosion damages on steel bar embedded in a) FA8, b) S3a-661 and c) MK2 mortar after 17 cycles of exposure.

4 CONCLUSIONS

In this study corrosion properties of steel exposed to different alkali-activated material environments, i.e. solid mortars and their pore solutions, is presented. The following conclusions can be made:

- Measurements in simulated pore solution using linear polarisation resistance (LPR) technique, electrical impedance spectroscopy (EIS) and cyclic potentiodynamic polarization (CPD) scans show similar results, namely steel in MK2 (metakaolin) pore solution is the most corrosion resistant and steel in S3a-661 (slag) pore solution is the least corrosion resistant. The distinction of corrosion properties between different pore solutions can also be observed from the results of the used electrochemical techniques. These differences could be more expressed if chlorides were present.

- Initial corrosion rates (ν_{corr}) of steel measured in solid mortars differ significantly from corrosion rates measured in their pore solutions. It is assumed that the steel/mortar interface properties and locally separated anodic and cathodic areas play significant role in corrosion processes of steel in alkali-activated mortars, which cannot be completely explained by simplified pore solution conditions. In time of exposure, these differences are more significant due to the presence of Cl^- ions.

- Electrochemical measurements were complemented by visual inspection, which provides information on corrosion type and therefore real corrosion damage areas which should be considered with interpretation of measured results.

- Methods which distinguish type of corrosion damages should be used for a comprehensive understanding of corrosion mechanisms in alkali-activated mortars. The use of X-ray computed microtomography should also be considered as a method complementary to electrochemical methods.

ACKNOWLEDGMENTS

The work described in this paper forms parts of the bilateral research project "Phenomenological modelling of steel corrosion in concretes for service life prediction", financed by Slovenian Research Agency (ARRS) and the French Alternative Energies and Atomic Energy Commission (CEA). Financial support of the Slovenian Research Agency (ARRS) through the research programme P2-0273 "Building structures and materials" is gratefully acknowledged.

REFERENCES

[1] Scrivener, K.L.; Kirkpatrick, R.J.: Innovation in Use and Research on Cementitious Material, *Cement and Concrete Research*, 38 (2008) 128–136
[2] Van Deventer, J.S.J.: Chapter 10 - Progress in the Adoption of Geopolymer Cement. In: *Handbook of Low Carbon Concrete*, Butterworth-Heinemann, (2017), pp. 217–262
[3] Provis, J.L.; Bernal, S.A.: Geopolymers and Related Alkali-Activated Materials. *Annu. Rev. Mater. Res.*, 44 (2014) 299–327
[4] Provis, J.L.: Alkali-Activated Materials, *Cement and Concrete Research*, 114 (2018) 40–48
[5] Criado, M.; Provis, J.L. Alkali Activated Slag Mortars Provide High Resistance to Chloride-Induced Corrosion of Steel, *Frontiers in Materials*, (2018) 5
[6] Alonso, C. et al.: Relation between Resistivity and Corrosion Rate of Reinforcements in Carbonated Mortar Made with Several Cement Types, *Cement and Concrete Research*, 18 (1988) 687–698
[7] Kelly, R.G. et al.: *Electrochemical Techniques in Corrosion Science and Engineering*, Marcel Dekker, Inc. (2003)
[8] Provis, J.L. et al.: RILEM TC 247-DTA Round Robin Test: Mix Design and Reproducibility of Compressive Strength of Alkali-Activated Concretes, *Mater Struct*, 52 (2019) 99
[9] Gluth, G.J.G. et al.: RILEM TC 247-DTA Round Robin Test: Carbonation and Chloride Penetration Testing of Alkali-Activated Concretes, *Mater Struct*, 53 (2020) 21
[10] Winnefeld, F. et al.: RILEM TC 247-DTA Round Robin Test: Sulfate Resistance, Alkali-Silica Reaction and Freeze–Thaw Resistance of Alkali-Activated Concretes, *Mater Struct*, 53 (2020) 140
[11] Gluth, G.; Rickard, W.: Design and Characterization of Fly Ash-Based Geopolymer Concretes for a Round-Robin Durability Testing Program In: *Proceedings of the Geopolymers: the route to eliminate waste and emissions in ceramic and cement manufacturing,* Engineering Conferences International / Società Ceramica Italiana: Hernstein, Austria, (2015), pp. 67–70
[12] Technical Committee CEN/TC 51. European Standard EN 196-1, *Methods of Testing Cement - Part 1: Determination of Strength*, European Committee for Standardization: Brussels, Belgium, (2016)
[13] Technical Committee ECISS/TC 100. European Standard EN 10027-2, *Designation Systems for Steels - Part 2: Numerical System*, European Committee for Standardization: Brussels, Belgium, (2015)
[14] Schiegg, Y. Monitoring of Corrosion in Reinforced Concrete Structures. In: *Corrosion in Reinforced Concrete Structures*, Woodhead Publishing Limited: Cambridge, England, (2005), pp. 46–70
[15] Cyr, M.; Daidié, A. Optimization of a High-Pressure Pore Water Extraction Device, *Review of Scientific Instruments*, 78 (2007) 023906
[16] Cyr, M. et al.: A. High-Pressure Device for Fluid Extraction from Porous Materials: Application to Cement-Based Materials, *Journal of the American Ceramic Society*, 91 (2008) 2653–2658